

## **Star Configuration based Control Method for Transformerless H-Bridge Cascaded Statcom by Fuzzy Logic**

**S.S. Deekshit<sup>1</sup>**

*Assistant Professor, Dept. Of EEE, AITS, Rajampet,*

**S.Sanjeeva Rayudu<sup>2</sup>**

*Assistant Professor, Dept. Of EEE, AITS, Rajampet,*

**Y.Nagendra<sup>3</sup>**

*PG Student, Dept. Of EEE, AITS, Rajampet,*

### **Abstract**

This paper displays a transformer less static synchronous compensator (STATCOM) framework in light of multilevel H-span converter with star design. The proposed control strategy is dedicating them to the present circle control as well as to the dc capacitor voltage control. With respect to the present circle control, a nonlinear controller in view of the lack of involvement based control (PBC) hypothesis is utilized as a part of this structure STATCOM surprisingly. With regards to the dc capacitor voltage control, general voltage control is acknowledged by embracing a corresponding full controller. Bunched adjusting control is acquired by utilizing a dynamic aggravations dismissal controller. Singular adjusting control is accomplished by moving the regulation wave vertically which can be effectively executed in a field-programmable door exhibit. Two genuine H-span fell STATCOMs appraised at 10 kV 2 MVA are developed and a progression of check tests are executed. Here fuzzy logic is used for controlling and compared with other controller the simpered systems tool has proved that the combined system will at the same time inject maximum power and provide dynamic frequency support to the grid. The trial results demonstrate that H-span fell STATCOM with the proposed control strategies has fantastic element execution and solid

heartiness. The dc capacitor voltage can be kept up at the given esteem successfully.

**Keywords:** Active disturbances rejection controller (ADRC), H-bridge cascaded, passivity-based control (PBC), proportional resonant (PR) controller, shifting modulation wave, static synchronous compensator (STATCOM).

## **I. INTRODUCTION**

FLEXIBLE ac transmission systems (FACTS) are being increasingly used in power system to enhance the system utilization, power transfer capacity as well as the power quality of ac system interconnections [1], [2]. As a typical shunt FACTS device, static synchronous compensator (STATCOM) is utilized at the point of

Normal association (PCC) to assimilate or infuse the required responsive force, through which the voltage nature of PCC is moved forward. As of late, numerous topologies have been connected to the STATCOM. Among these distinctive sorts of topology, H-span fell STATCOM has been broadly acknowledged in high-control applications for the accompanying focal points: snappy reaction speed, little volume, high effectiveness, insignificant collaboration with the supply lattice and its individual stage control capacity. Contrasted and a diode-clinched converter or flying capacitor converter, H-span fell STATCOM can acquire a high number of levels all the more effortlessly and can be associated with the network straightforwardly without the massive transformer. This empowers us to diminish cost and enhance execution of H-extension fell STATCOM.

There are two specialized difficulties which exist in H-span fell STATCOM to date. To begin with, the control strategy for the present circle is an essential component affecting the pay execution. Notwithstanding, numerous non-perfect variables, for example, the constrained data transfer capacity of the yield current circle, the time delay instigated by the sign identifying circuit, and the reference charge current era procedure, will break down the pay impact. Second, H-span fell STATCOM is a confused framework with numerous H-span cells in every stage, so the dc capacitor voltage unevenness issue which brought about by various

Dynamic force misfortunes among the cells, distinctive exchanging designs for various cells, parameter varieties of dynamic and latent segments inside cells will impact the dependability of the framework and even prompt the breakdown of the framework. Consequently, bunches of inquires about have concentrated on looking for the answers for these issues.

## II. CONFIGURATION OF THE 10 KV 2 MVA STATCOM SYSTEM

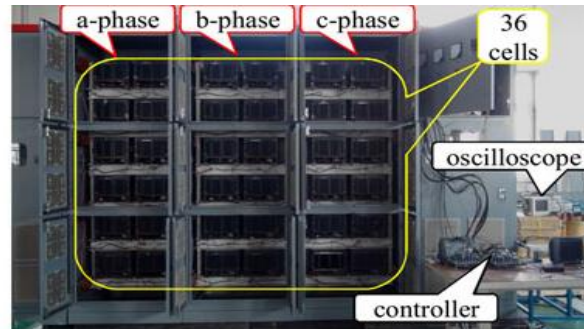


**Fig.1 (a):** Actual 10kV 2MVA H-bridge cascaded STATCOM hardware view.

Fig. 1 shows the circuit configuration of the 10 kV 2 MVA star-configured STATCOM cascading 12 H-bridge pulse width modulation (PWM) converters in each phase and it can be expanded easily according to the requirement. By controlling the current of STATCOM directly, it can absorb or provide the required reactive current to achieve the purpose of dynamic reactive current compensation. Finally, the power quality of the grid is improved and the grid offers the active current only. The power switching devices working in ideal condition is assumed.  $u_{sa}$ ,  $u_{sb}$ , and  $u_{sc}$  are the three-phase voltage of grid.  $u_a$ ,  $u_b$ , and  $u_c$  are the three-phase voltage of STATCOM.  $i_{sa}$ ,  $i_{sb}$ , and  $i_{sc}$  are the three-phase current of grid.  $i_a$ ,  $i_b$ , and  $i_c$  are the three-phase current of STATCOM.  $i_{la}$ ,  $i_{lb}$ , and  $i_{lc}$  are the three-phase current of load.  $U_{dc}$  is the reference voltage of dc capacitor.  $C$  is the dc capacitor.  $L$  is the inductor.  $R_s$  is the starting resistor.

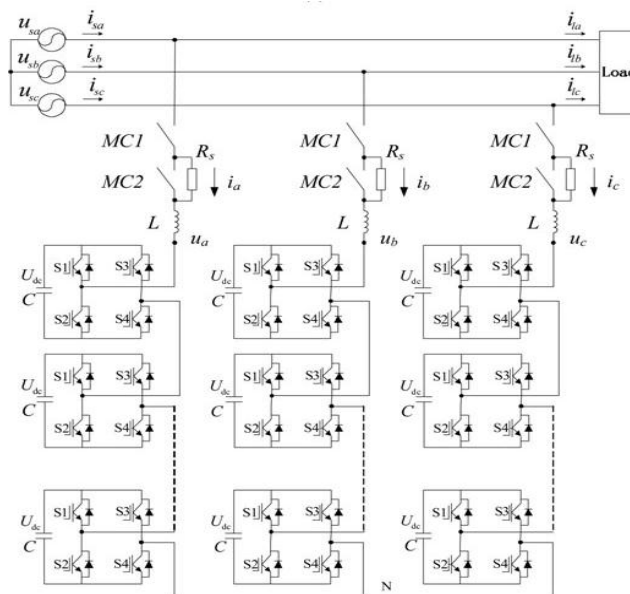


**Fig.1 (b):** Actual 10kV 2MVA H-bridge cascaded STATCOM configuration system.

**TABLE I**  
CIRCUIT PARAMETERS OF THE EXPERIMENTAL SYSTEM

Grid voltage	$u_s$	10 kV
Rated reactive	$Q$	2 MVA
AC inductor	$L$	10 mH
Starting resistor	$R_s$	4 k $\Omega$
DC capacitor capacitance	$C$	5600 $\mu$ F
DC capacitor reference voltage	$U_{dc}$	800 V
Number of H-bridges	$N$	12
PWM carrier frequency	$f$	1 kHz

The modulation technology adopts the carrier phase-shifted sinusoidal PWM (abbreviated as CPS-SPWM) with the carrier frequency of 1 kHz. Then, with a cascade number of  $N = 12$ , the ac voltage cascaded results in a 25-level waveform in line to neutral and a 49-level waveform in line to line. In each cluster carrier signals with the same frequency as 1 kHz are phase shifted by  $2\pi/12$  from each other. When a carrier frequency is as low as 1 kHz, using the method of phase-shifted unipolar sinusoidal PWM, it can make an equivalent carrier frequency as high as 24 kHz.

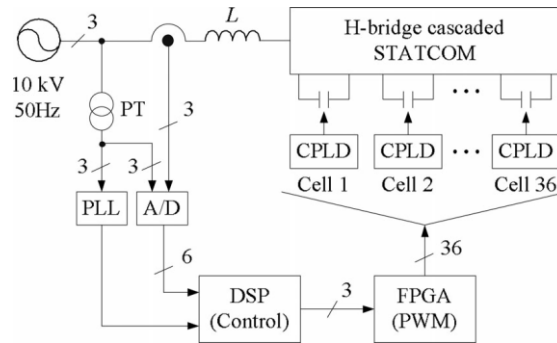


**Fig.2:** Digital control system for 10 kV 2 MVA H-bridge cascaded STATCOM.

### III. CONTROL ALGORITHM

Fig. 3 shows a block diagram of the control algorithm for H-bridge cascaded STATCOM. The whole control algorithm mainly consists of four parts, namely, PBC, overall voltage control, clustered balancing control, and individual balancing control. The first three parts are achieved in DSP, while the last part is achieved in the FPGA.

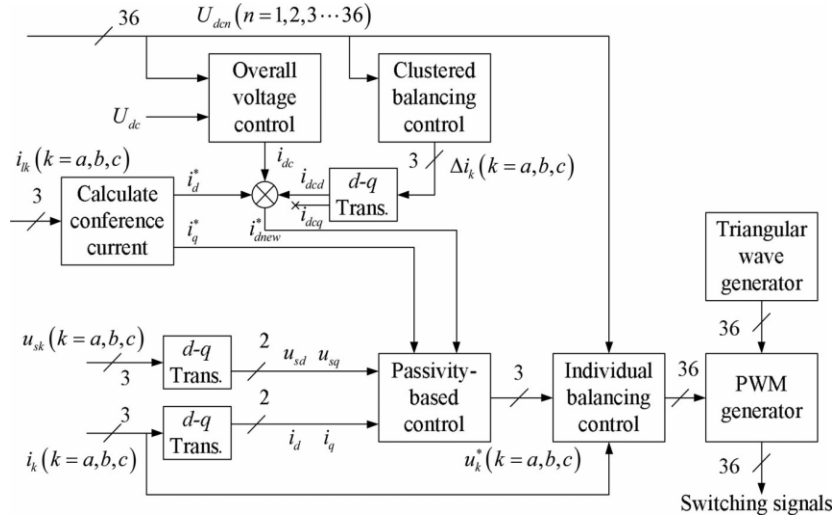


**Fig.3:** Control block diagram for the 10 kV 2 MVA H-bridge cascaded STATCOM.

#### A. PBC:

Referring to Fig. 1, the following set of voltage and current equations can be derived:

$$L \frac{di_a}{dt} = u_{sa} - u_a - Ri_a$$

$$L \frac{di_b}{dt} = u_{sb} - u_b - Ri_b$$

$$L \frac{di_c}{dt} = u_{sc} - u_c - Ri_c \quad (1)$$

Where  $R$  is the equivalent series resistance of the inductor. Applying the  $d-q$  transformations (1), the equations in  $d-q$  axis are obtained

$$L \frac{di_d}{dt} = -Ri_d + \omega Li_q + u_{sd} - u_d$$

$$L \frac{di_q}{dt} = -Ri_q - \omega Li_d + u_{sq} - u_q \quad (2)$$

Equation (2) is written as the following form:

$$\begin{aligned} & \begin{bmatrix} L & 0 \\ 0 & L \end{bmatrix} \begin{bmatrix} \frac{di_d}{dt} \\ \frac{di_q}{dt} \end{bmatrix} + \begin{bmatrix} 0 & -\omega L \\ \omega L & 0 \end{bmatrix} \begin{bmatrix} i_d \\ i_q \end{bmatrix} + \begin{bmatrix} R & 0 \\ 0 & R \end{bmatrix} \begin{bmatrix} i_d \\ i_q \end{bmatrix} \\ & = \begin{bmatrix} u_{sd} & -u_d \\ u_{sq} & -u_q \end{bmatrix} \end{aligned} \quad (3)$$

Along with selecting  $id$  and  $iq$  as state variables, it gives the following EL system model of (3):

$$M\dot{X} + JX + RX = u \quad (4)$$

Where  $x = [id \ iq]$  is the state variable.

$M = [L \ 0 \ 0 \ L]$  is the positive definite inertial matrix and

$\mathbf{M} = \mathbf{M}^T$ .  $J = [0 \ -\omega L \ \omega L \ 0]$  is the dissymmetry interconnection matrix and

$\mathbf{J} = -\mathbf{J}^T$ .  $R = [R \ 0 \ 0 \ R]$  is the positive definite symmetric matrix which reflects the dissipation characteristic of the system.

$u = u_{sd} - u_{dsq} - u_{qis}$  is the external input matrix which reflects the energy exchange between the system and environment.

$$V = \frac{1}{2} X^T M X - Q(x) \quad (5)$$

Assume the energy storage function as (6) for H-bridge cascaded STATCOM

$$V = \frac{1}{2} X^T M X = \frac{1}{2} L (i_d^2 + i_q^2) \quad (6)$$

By taking the derivative of  $V$  and utilizing anti symmetric characteristic of  $\mathbf{J}$ , (7) is obtained as follows:

$$\dot{V} = X^T M \dot{X} = X^T (u - JX - RX) = X^T u - X^T R X \quad (7)$$

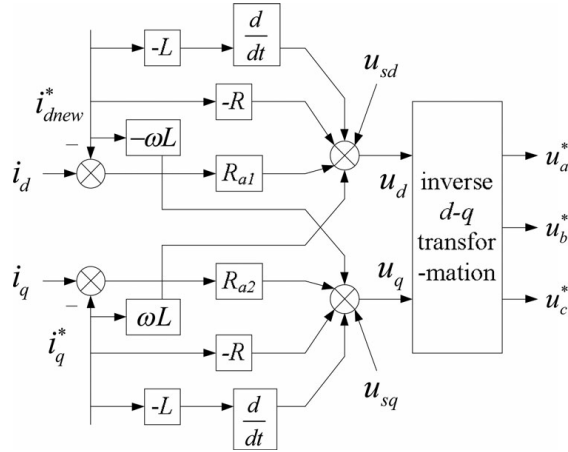


**Fig.4:** Block diagram of PBC.

### B. Overall Voltage Control

As the main level control of the dc capacitor voltage adjusting, the point of the general voltage control is to keep the dc mean voltage of all converter cells

approaching to the dc capacitor reference voltage. The normal methodology is to embrace the routine PI controller which is easy to actualize. In any case, the yield voltage and current of H-scaffold fell STATCOM are the force recurrence sinusoidal variables and the yield force is the twofold power recurrence sinusoidal variable, it will make the dc capacitor likewise has the twofold power recurrence swell voltage. In this way, the reference current which is gotten during the time spent the general voltage control is not a standard dc variable and it likewise has the twofold power recurrence rotating part and it will decrease the nature of STATCOM yield current.

$$G_{PR}(s) = k_p + \frac{2k_r\omega_c s}{s^2 + 2\omega_c s + \omega_0^2} \tag{8}$$

Where  $k_p$  is the proportional gain coefficient.  $k_r$  is the integral gain coefficient.  $\omega_c$  is the cutoff frequency.  $\omega_0$  is the resonant frequency.  $k_r$  influences the gain of the controller but the bandwidth. With  $k_r$  increasing, the amplitude at the resonant frequency is also increased and it plays a role in the elimination of the steady-state error.  $\omega_c$  influences the gain of the controller and the bandwidth.

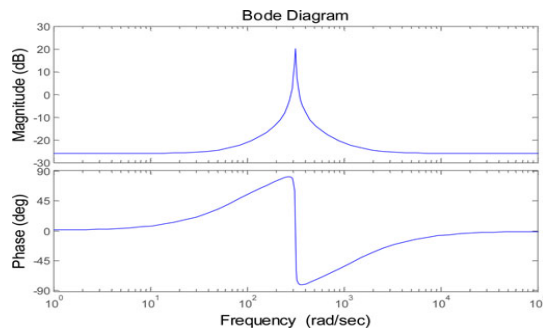


**Fig.5:** Bode plots of the PR controller.

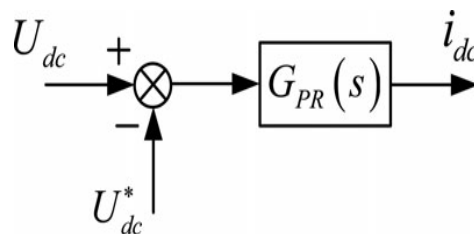


**Fig.6:** Block diagram of overall voltage control.

**C. Clustered Balancing Control**

Taking the clustered balancing control as the second level control of the dc capacitor voltage balancing, the purpose is to keep the dc mean voltage of 12 cascaded converter cells in each cluster equaling the dc mean voltage of the three clusters. ADRC is adopted to achieve it.

- 1) H-bridge cascaded STATCOM is a first order system; thus, the first-order ADRC is designed. Taking the dc capacitor voltage of each cluster as the controlled object for analysis, the clustered balancing control model is built and the input and output variables and the controlled variable of the controlled object are determined.
- 2) By using the nonlinear tracking differentiator (TD) which is a component of ADRC, the transient process for the reference input of the controlled object is arranged and its differential signal is extracted.

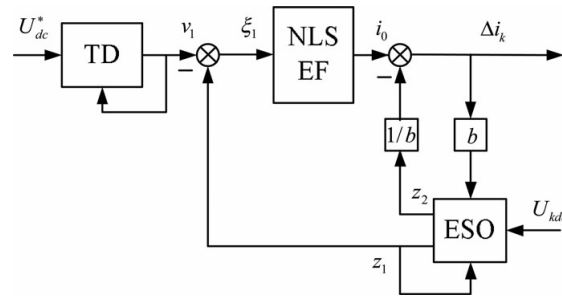


**Fig.7:** Block diagram of clustered balancing control.

#### D. Individual Balancing Control

As the overall dc voltage and the clustered dc voltage are controlled and maintained, the individual control becomes necessary because of the different cells have different losses. The aim of the individual balancing control as the third level control is to keep each of 12 dc voltages in the same cluster equaling to the dc mean voltage of the corresponding cluster. It plays an important role in balancing 12 dc mean capacitor voltages in each cluster.

Due to the symmetry of structure and parameters among the three phases, a-phase cluster is taken as an example for the individual balancing control analysis. Fig. 8 shows the charging and discharging states of one cell. According to the polarity of output voltage and current of the cell, the state of the dc capacitor can be judged. Then, the dc capacitor voltage will be adjusted based on the actual voltage value.

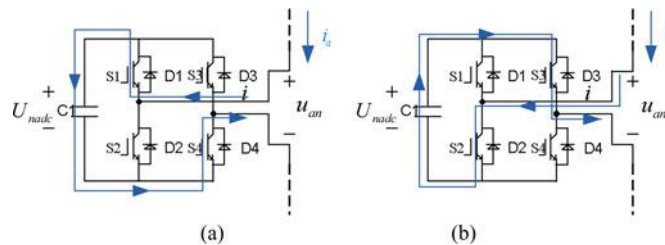


**Fig.8:** Charging and discharging states of one cell.  
(a) Charging state. (b) Discharging state.

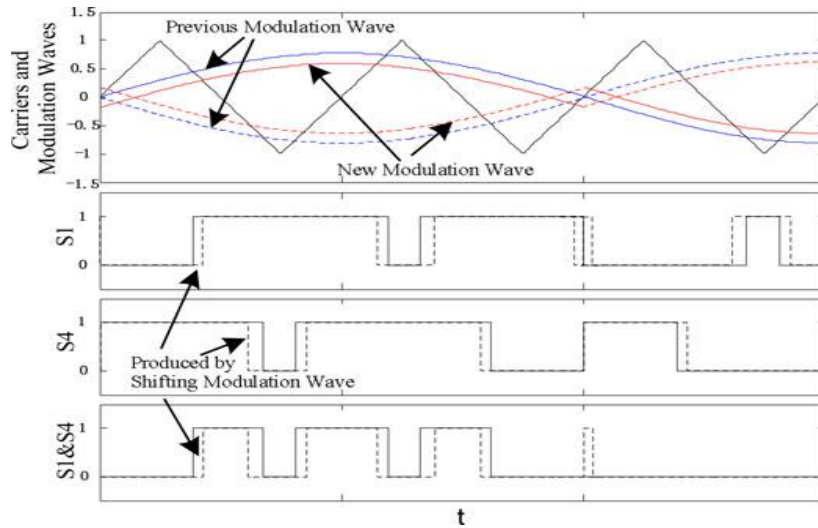


**Fig.9:** Process of shifting modulation wave.

The previous principle is also suitable for reducing discharging time and prolonging the charging and discharging times of the cell. Summing up the previous analysis, the method can be illustrated as follows. 1) If the requirement is to reduce the duty cycle, it needs to shift down the normal modulation wave and shift up the opposite modulation wave. 2) If the requirement is to prolong the duty cycle, it needs to shift up the normal modulation wave and shift down the opposite modulation wave.

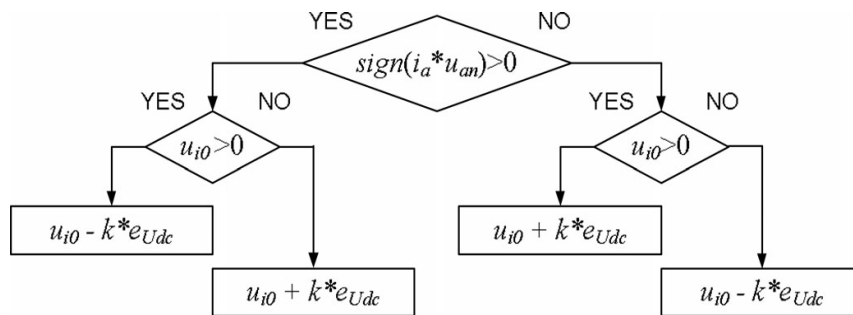


**Fig.10:** Flowchart of shifting modulation wave.

#### IV. FUZZY LOGIC CONTROL

The Fuzzy logic control consists of set of linguistic variables. Here the PI controller is replaced with Fuzzy Logic Control. The mathematical modeling is not required in FLC. FLC consists of

##### 1. Fuzzification

Membership function values are assigned to linguistic variables. In this scaling factor is between 1 and -1.

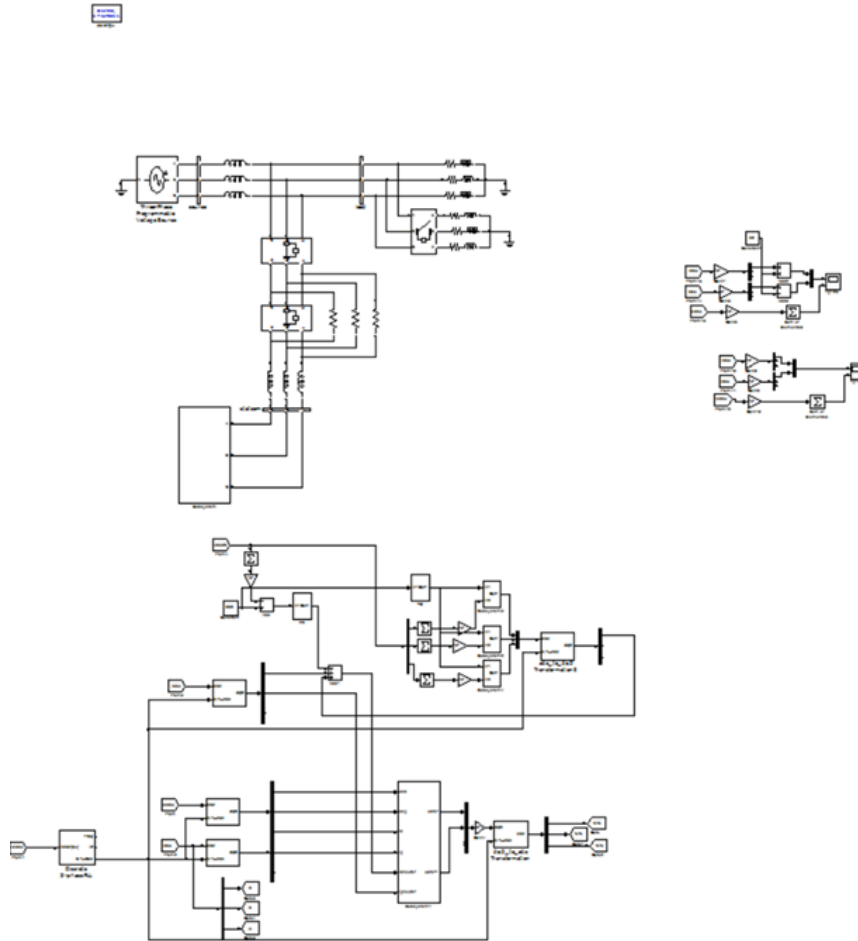


**Fig.11:** Simulated diagram by fuzzy logic controller.

### 2. Inference Method

There are several composition methods such as Max-Min and Max-Dot have been proposed and Min method is used.

### 3. Defuzzification

A plant requires non fuzzy values to control, so defuzzification is used. The output of FLC controls the switch in the inverter. To control these parameters they are sensed and compared with the reference values. To obtain this the membership functions of fuzzy controller are shown in fig (7).

The set of FC rules are derived from

$$u = -[\alpha E + (1-\alpha)C] \quad (9)$$

Where  $\alpha$  is self-adjustable factor which can regulate the whole operation.  $E$  is the error of the system,  $C$  is the change in error and  $u$  is the control variable. A large value of error  $E$  indicates that given system is not in the balanced state. If the system

is unbalanced, the controller should enlarge its control variables to balance the system as early as possible.

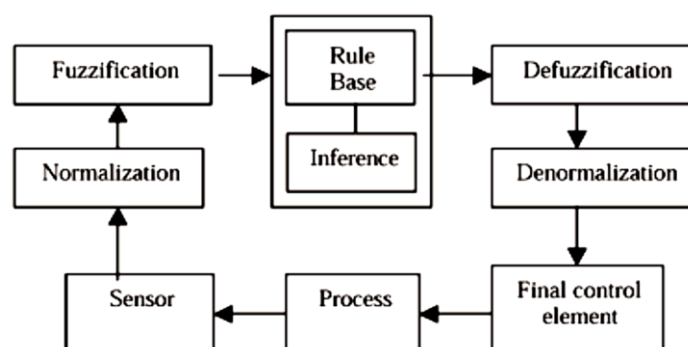


**Fig.12:** Fuzzy logic Controller

## V. SIMULATION RESULTS

To verify the correctness and effectiveness of the proposed methods, the simulation platform is built according to the second part of this paper by using fuzzy logic controller. Two H-bridge cascaded STATCOMs are running simultaneously. One generates the set reactive current and the other generates the compensating current that prevents the reactive current from flowing into the grid. The simulation is divided into two parts: the current loop control simulation and the dc capacitor voltage balancing control simulation. In current loop control simulation, the measured simulational waveform is the current of a-phase cluster and it is recorded by the oscilloscope. In dc capacitor voltage balancing control simulation, the value of dc capacitor voltages are transferred into DSP by a signal acquisition system and they can be recorded and observed by CCS software in computer. Finally, with the exported experimental data from CCS, experimental waveform is plotted by using MATLAB by using fuzzy logic controller.

### A. Current Loop Control:

The current loop control simulation is divided into four processes: steady-state process, dynamic process, startup process, and stopping process Fig. 13 shows the simulation results verifying the effect of PBC in steady-state process. As shown in Fig. 13(a), it is the simulation result of the full load test. With the proposed control method, the reactive current is compensated effectively. The error of the compensation is very small. The residual current of the grid is also quite small. The waveforms of the compensating current and the reactive current are smooth and they have the small distortion and the great sinusoidal shape. As shown in Fig. 13(b), it is the simulation result of the over load test. When STATCOM is running in over load state (about 1.4 times current rating), due to the selected IGBT has been reserved the enough safety margin, STATCOM still can run continuously and steadily. The over load capability of STATCOM is improved greatly and the operating reliability of

STATCOM in practical industrial field is enhanced effectively. However, considering the over load capability of other devices.

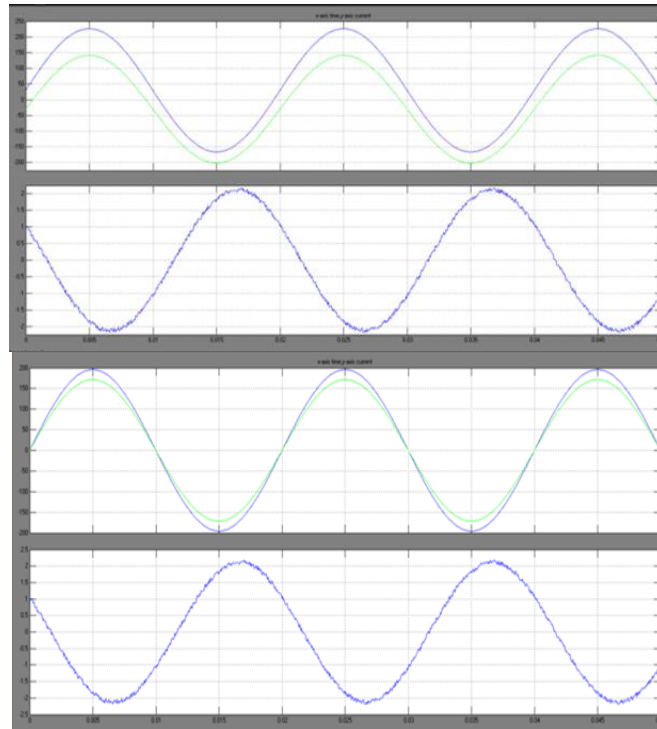


**Fig.13.** Simulated results verify the effect of PBC in steady-state process. (a) Ch1: reactive current; Ch2: compensating current; Ch3: residual current of grid. (b) Ch1: reactive current; Ch2: compensating current; Ch3: residual current of grid.

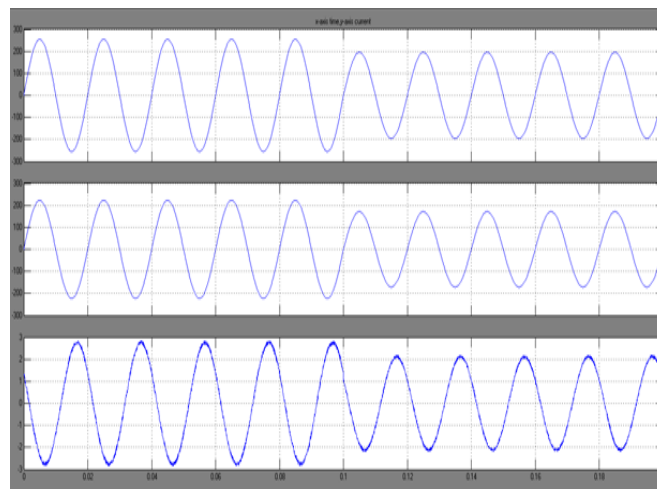


**Fig.14.** Simulated results show the dynamic performance of STATCOM in the dynamic process. Ch1: reactive current; Ch2: compensating current; Ch3: residual current of grid

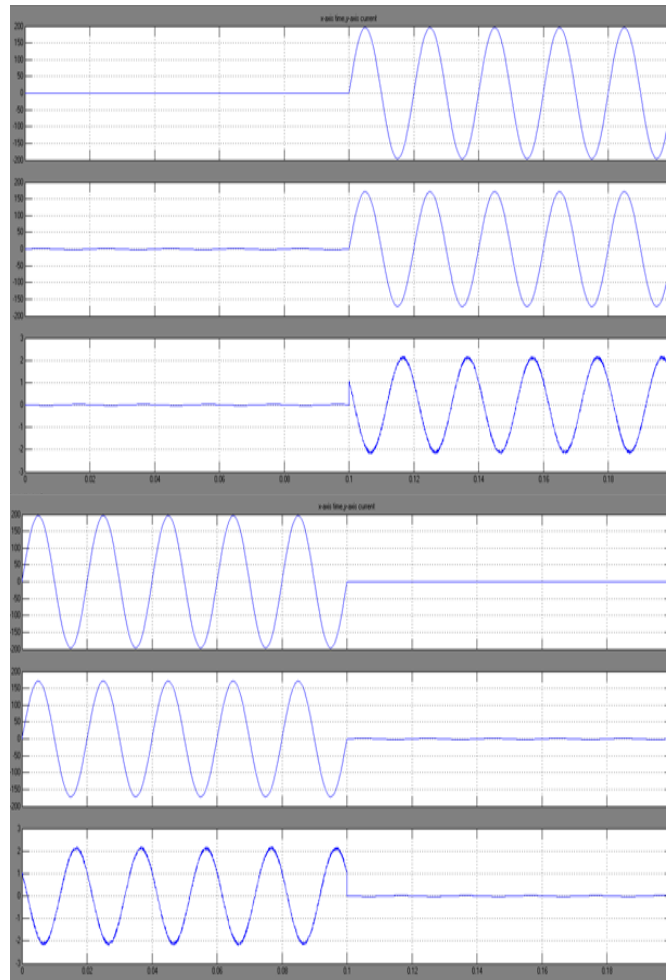


**Fig.15.** Simulated results in the startup process and stopping process. (a) Ch1: reactive current; Ch2: compensating current; Ch3: residual current of grid. (b) Ch1: reactive current; Ch2: compensating current; Ch3: residual current of grid.

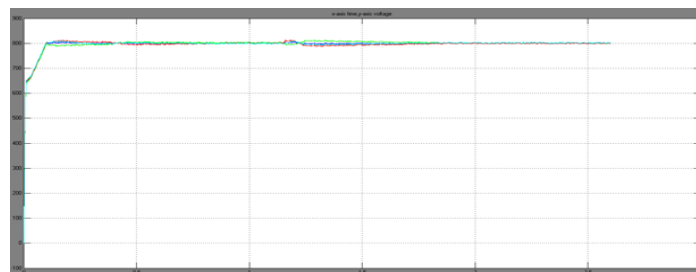


**Fig.16:** Simulated waveforms for testing clustered balancing control in the startup process and dynamic process. DC mean voltage of all converter cells  $U_{*dc}$ ; dc mean voltage  $U_k dc$  ( $k = a, b, c$ ) of 12 cascaded converter cells in each cluster.

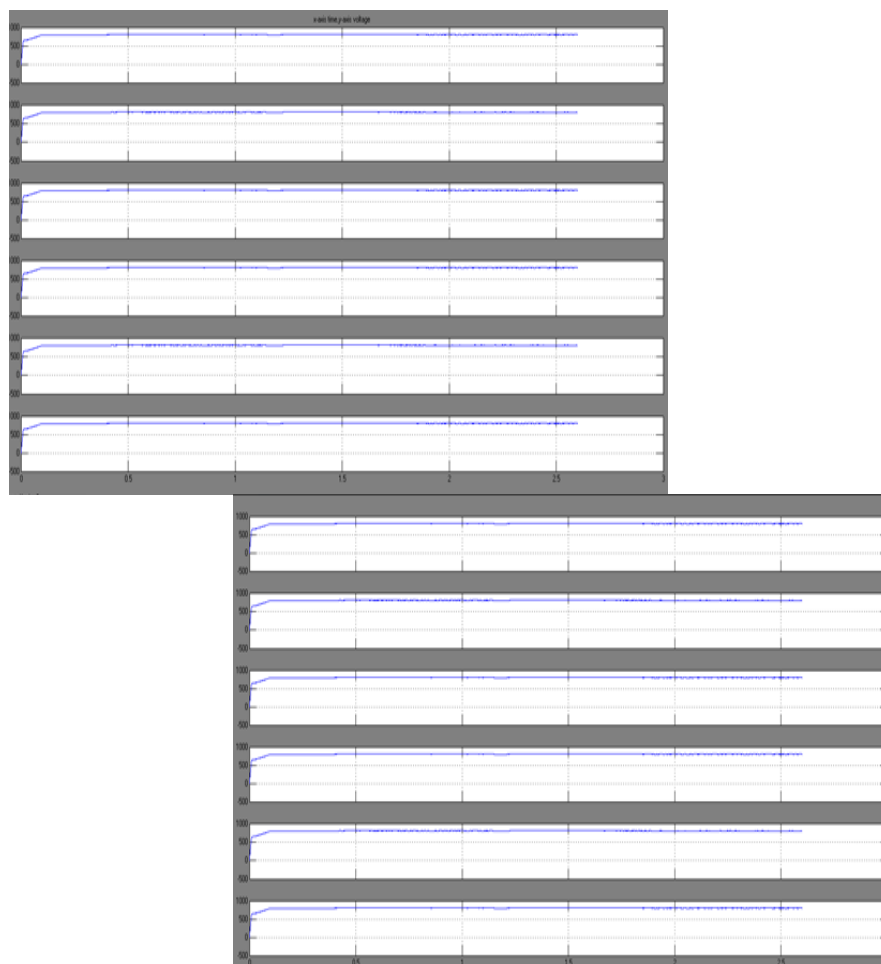


**Fig. 17.** Simulated waveforms of 12 cells in a-phase cluster for testing individual balancing control in the steady-state process.

## VI. CONCLUSION

This paper has investigated the basics of STATCOM in light of multilevel H-span converter with star setup by fluffy. And after that, the real H-span fell STATCOM evaluated at 10 kV 2 MVA is developed and the novel control strategies are additionally proposed in point of interest. The MATLAB/Simpower frameworks recreation indicates sensible exhibitions of this controller. Here fluffy controller is utilized contrasted with option controllers due to its exact execution. The proposed strategies have the accompanying attributes.

1) A PBC hypothesis based nonlinear controller is initially utilized as a part of STATCOM with this fell structure for the present circle control, and the feasibility is confirmed by the test results.

2) The PR controller is intended for general voltage control and the test result demonstrates that it has better execution regarding reaction time and damping profile contrasted and the PI controller.

3) The ADRC is initially utilized as a part of H-scaffold fell STATCOM for grouped adjusting control and the trial results check that it can understand fantastic element remuneration for the outside unsettling influence.

4) The individual adjusting control technique which is acknowledged by moving the regulation wave vertically can be effortlessly executed in the FPGA.

The reproduced results have affirmed that the proposed strategies are plausible and compelling. What's more, the discoveries of this study can be stretched out to the control of any multilevel voltage source converter, particularly those with H-span fell structure.

## REFERENCES

- [1] B. Gultekin and M. Ermis, "Cascaded multilevel converter-based transmission STATCOM: System design methodology and development of a 12 kV  $\pm$ 12 MVar power stage," *IEEE Trans. Power Electron.*, vol. 28, no. 11, pp. 4930–4950, Nov. 2013.
- [2] B. Gultekin, C. O. Gerc¸ek, T. Atalik, M. Deniz, N. Bic¸er, M. Ermis, K. Kose, C. Ermis, E. Koc¸, I. C¸adirci, A. Ac¸ik, Y. Akkaya, H. Toygar, and S. Bideci, "Design and implementation of a 154-kV $\pm$ 50-Mvar transmission STATCOM based on 21-level cascaded multilevel converter," *IEEE Trans. Ind. Appl.*, vol. 48, no. 3, pp. 1030–1045, May/Jun. 2012.
- [3] S. Kouro, M. Malinowski, K. Gopakumar, L. G. Franquelo, J. Pou, J. Rodriguez, B. Wu, M. A. Perez, and J. I. Leon, "Recent advances and industrial applications of multilevel converters," *IEEE Trans. Ind. Electron.*, vol. 57, no. 8, pp. 2553–2580, Aug. 2010.
- [4] F. Z. Peng, J.-S. Lai, J. W. McKeever, and J. VanCoevering, "A multilevel voltage-source inverter with separate DC sources for static var generation," *IEEE Trans. Ind. Appl.*, vol. 32, no. 5, pp. 1130–1138, Sep./Oct. 1996.
- [5] Y. S. Lai and F. S. Shyu, "Topology for hybrid multilevel inverter," *Proc. Inst. Elect. Eng.—Elect. Power Appl.*, vol. 149, no. 6, pp. 449–458, Nov. 2002.
- [6] D. Soto and T. C. Green, "A comparison of high-power converter topologies for the implementation of FACTS controllers," *IEEE Trans. Ind. Electron.*, vol. 49, no. 5, pp. 1072–1080, Oct. 2002.

- [7] C. K. Lee, J. S. K. Leung, S. Y. R. Hui, and H. S.-H. Chung, "Circuit-level comparison of STATCOM technologies," *IEEE Trans. Power Electron.*, vol. 18, no. 4, pp. 1084–1092, Jul. 2003.
- [8] H. Akagi, S. Inoue, and T. Yoshii, "Control and performance of a transformerless cascade PWM STATCOM with star configuration," *IEEE Trans. Ind. Appl.*, vol. 43, no. 4, pp. 1041–1049, Jul./Aug. 2007.
- [9] A. H. Norouzi and A. M. Sharaf, "Two control scheme to enhance the dynamic performance of the STATCOM and SSSC," *IEEE Trans. Power Del.*, vol. 20, no. 1, pp. 435–442, Jan. 2005.
- [10] C. Schauder, M. Gernhardt, E. Stacey, T. Lemak, L. Gyugyi, T. W. Cease, and A. Edris, "Operation of  $\pm 100$  MVar TVA STATCOM," *IEEE Trans. Power Del.*, vol. 12, no. 4, pp. 1805–1822, Oct. 1997.
- [11] C. H. Liu and Y. Y. Hsu, "Design of a self-tuning PI controller for a STATCOM using particle swarm optimization," *IEEE Trans. Ind. Electron.*, vol. 57, no. 2, pp. 702–715, Feb. 2010.
- [12] S. Mohagheghi, Y. Del Valle, G. K. Venayagamoorthy, and R. G. Harley, "A proportional-integrator type adaptive critic design-based neurocontroller for a static compensator in a multimachine power system," *IEEE Trans. Ind. Electron.*, vol. 54, no. 1, pp. 86–96, Feb. 2007.
- [13] H. F. Wang, H. Li, and H. Chen, "Application of cell immune response modelling to power system voltage control by STATCOM," *Proc. Inst. Elect. Eng. Gener. Transm. Distrib.*, vol. 149, no. 1, pp. 102–107, Jan. 2002.
- [14] A. Jain, K. Joshi, A. Behal, and N. Mohan, "Voltage regulation with STATCOMs: Modeling, control and results," *IEEE Trans. Power Del.*, vol. 21, no. 2, pp. 726–735, Apr. 2006.
- [15] V. Spitsa, A. Alexandrovitz, and E. Zeheb, "Design of a robust state feedback controller for a STATCOM using a zero set concept," *IEEE Trans. Power Del.*, vol. 25, no. 1, pp. 456–467, Jan. 2010.

#### **AUTHOR'S PROFILE:**

**S. SRIKANTA DEEKSHIT:** Currently, he is working as an assistant professor in the Department of Electrical & Electronics Engineering, Annamacharya institute of technology and science, Rajampet (AITS), Andhra Pradesh, India. He received the B.E. degree in Electrical and Electronics Engineering (EEE), with distinction from the Sri Chandra sekharendra Saraswathi ViswaMaha Vidyalaya (SCSVMV) University, Kancheepuram (DT), Tamilnadu in 2012, He received the Master Degree in Electrical Power Systems (EPS) at Madanapalle Institute Of Technology & Science (MITS), Angallu- 517325, Chittoor (DT), Andhra Pradesh, India in 2014.

**S.SANJEEVA RAYUDU:** Currently, he is working as an assistant professor in the Department of Electrical & Electronics Engineering, Annamacharya institute of technology and science, Rajampet (AITS), Andhra Pradesh, India. He received the B.E. degree in Electrical and Electronics Engineering (EEE), from the G Pulla Reddy Engineering College (GPREC), Kurnool (DT), Andhra Pradesh in 2012. He received the Master Degree in Power Electronics (PE) at National Institute of Technology (NIT), Tiruchirappali-620015, Tamilnadu, India in 2014.

**Y.NAGENDRA:** He was born in 1992. He obtained his Bachelor degree in Electrical and Electronics Engineering in 2014 from NIST, Rajampet. Currently pursuing his Post Graduation in Electrical Power Engineering in AITS, Rajampet, Kadapa (dist.), Andhra Pradesh, India in 2016.

